Cross-frequency coupling supports multi-item working memory in the human hippocampus

Nikolai Axmacher[a,b,1], Melanie M. Henseler[a,c], Ole Jensen[d], Ilona Weinreich[c], Christian E. Elger[a,b], and Juergen Fell[a]

[a]Department of Epileptology, University of Bonn, Bonn 53105, Germany; [b]Life and Brain Center of Academic Research, Bonn 53105, Germany; [c]Department of Mathematics and Technology, University of Applied Sciences Koblenz, RheinAhrCampus Remagen, Remagen 53424, Germany; and [d]F.C. Donders Centre for Cognitive Neuroimaging, 6525 EN Nijmegen, The Netherlands

Edited by James L. McClelland, Stanford University, Stanford, CA, and approved December 29, 2009 (received for review October 6, 2009)

Recent findings indicate that the hippocampus supports not only long-term memory encoding but also plays a role in working memory (WM) maintenance of multiple items; however, the neural mechanism underlying multi-item maintenance is still unclear. Theoretical work suggests that multiple items are being maintained by neural assemblies synchronized in the gamma frequency range (25–100 Hz) that are locked to consecutive phase ranges of oscillatory activity in the theta frequency range (4–8 Hz). Indeed, cross-frequency coupling of the amplitude of high-frequency activity to the phase of slower oscillations has been described both in animals and in humans, but has never been linked to a theoretical model of a cognitive process. Here we used intracranial EEG recordings in human epilepsy patients to test pivotal predictions from theoretical work. First, we show that simultaneous maintenance of multiple items in WM is accompanied by cross-frequency coupling of oscillatory activity in the hippocampus, which is recruited during multi-item WM. Second, maintenance of an increasing number of items is associated with modulation of beta/gamma amplitude with theta band activity of lower frequency, consistent with the idea that longer cycles are required for an increased number of representations by gamma cycles. This effect cannot be explained by a difference in theta or beta/gamma power. Third, we describe how the precision of cross-frequency coupling predicts individual WM performance. These data support the idea that working memory in humans depends on a neural code using phase information.

Working memory (WM), the ability to maintain information about multiple items over a short time span, is indispensable for goal-directed behavior (1). Precise synchronization of neurons and neural networks results in oscillatory activity patterns in the gamma frequency range (25–100 Hz) and serves to facilitate neural communication and memory processing (2, 3). Data from animals and humans provide evidence that sustained increases of high-frequency activity (4–7) and theta (4–8 Hz) oscillations (8–10) are a neural correlate of WM maintenance. However, how multiple items can be simultaneously maintained without interference remains unknown. In animals, action potentials firing with respect to specific phases of ongoing theta oscillations accompany the encoding of sequences of spatial positions (11). In addition, firing rate is modulated by the phase of gamma band activity (12, 13). A related phase code based on interactions of theta phase and gamma oscillations has been suggested to support maintenance of multiple items in WM (14, 15). Such cross-frequency coupling has been described in rodents (16, 17) and recently in the human brain (18, 19), but its link to multi-item WM has not been investigated.

Here we address the question of whether multiple items are encoded by modulation of the amplitude of high-frequency oscillations by the phase of oscillations in a lower-frequency range in the human hippocampus. We used a modified Sternberg paradigm in which one, two, or four trial-unique novel faces were presented consecutively (Fig. S1). Oscillatory activity within the hippocampus, which has been shown to be specifically recruited during complex WM tasks involving multiple novel items or relational memory (7, 20, 21), was recorded in 14 epilepsy patients with bilateral hippocampal depth electrodes (*Methods*). Cross-frequency coupling of high-frequency amplitude to the phase of activity at lower frequency was quantified by calculating Pearson's cross-correlations between the analytic amplitude of high-frequency oscillations and the real part of wavelet-transformed oscillations at lower frequency, shifted by the average modulation phase Figs. S2–S4.

In particular, we addressed three questions derived from theoretical work. First, we studied whether WM maintenance in general was accompanied by increased coupling of gamma amplitude to theta phase as compared to baseline. Second, we tested whether maintenance of an increasing number of items results in a decreased frequency of the lower (modulating) oscillation—corresponding to longer individual theta cycles—and/or in a broader theta phase range during which gamma amplitude was enhanced (22). Finally, we investigated the behavioral relevance of theta-gamma coupling by analyzing the correlation of modulation parameters to individual performance. The analyses presented here are based on an extension (14 instead of 11 subjects) of a data sample described in an earlier article (7).

Results

First, we averaged across the different memory load conditions to investigate whether a distinct modulation of gamma amplitude by theta phase was apparent during successful WM maintenance (Fig. 1*A*) as compared to baseline (period of equal length in the intertrial interval; Fig. 1*B*). Cross-frequency coupling was enhanced in the range of 6–10 Hz (modulating frequency) versus 14–50 Hz (modulated frequency) with peaks at 7 versus 28 Hz. Fig. S5 *A–C* depicts modulation values across the entire frequency range that was subjected to the calculation, that is, between 14 and 200 Hz. This effect corresponds to a modulation of the amplitude of activity in the beta/gamma frequency range by the phase of activity in the theta range. Average modulation strength in these ranges was significantly higher during WM maintenance as compared to baseline (0.035 ± 0.011 vs. 0.022 ± 0.009; $t_{13} = 4.14$; $p_{corr} = 0.016$). Notably, we did not observe modulations across broader frequency ranges. It should be noted that the frequency ranges for this comparison were based on the WM maintenance alone and that the statistical test between WM maintenance and baseline was done subsequently. To corroborate this finding, we also compared modulation strength during WM maintenance with modulation strength in phase-scrambled surrogate data (Fig. 1*C*; see *Methods*); again, in these surrogate data, modulation strength was significantly reduced ($p_{corr} < 0.05$). Similarly, a second set of even more conservative surrogate data was constructed, in which the time series of both gamma power and theta phase were conserved but trials for gamma power and for theta phase were randomly attributed to each other (for each patient; see *SI Methods*

Author contributions: N.A., I.W., C.E.E., and J.F. designed research; N.A. and J.F. performed research; N.A., M.M.H., and J.F. analyzed data; and N.A., O.J., and J.F. wrote the paper.

The authors declare no conflict of interest.

This article is a PNAS Direct Submission.

[1]To whom correspondence should be addressed. E-mail: nikolai.axmacher@ukb.uni-bonn.de.

This article contains supporting information online at www.pnas.org/cgi/content/full/0911531107/DCSupplemental.

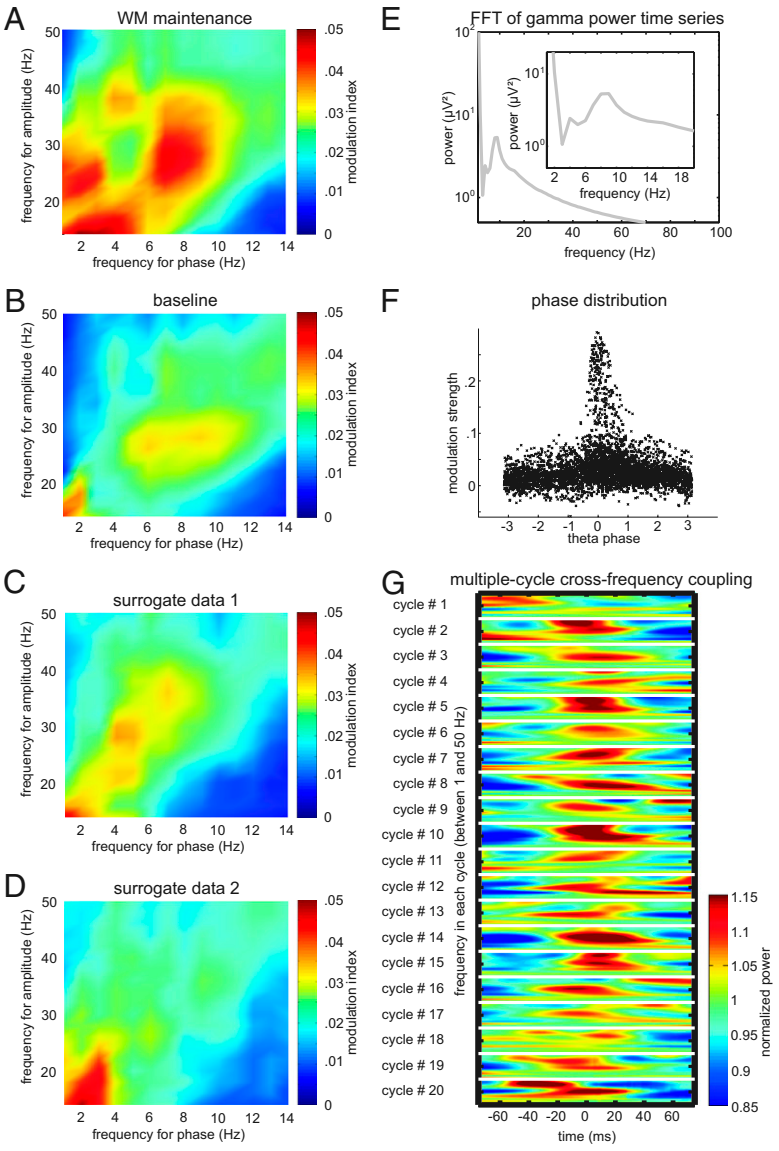

Fig. 1. Theta-beta/gamma modulation in the human hippocampus during working memory maintenance. Cross-frequency coupling during WM maintenance (*A*) was larger than during the baseline period (*B*) in the human hippocampus (all figures depict grand averages across subjects). Modulation peaked at 7 Hz for the lower-frequency (modulating) theta oscillations and at 28 Hz for the high (modulated) beta/gamma oscillations. (*C* and *D*) Cross-frequency coupling in scrambled surrogate data and in surrogate data obtained by randomly assigning trials for gamma power and trials for theta phase. (*E*) Remaining cross-frequency coupling in these surrogates can be explained by fluctuations of gamma power time series at theta frequency. FFT, fast Fourier transform. (*F*) Depiction of modulation strength at the phase for which modulation was maximal in each trial indicates that modulation of beta/gamma amplitude reaches its maximum at a theta phase around 0°. (*G*) Cross-frequency coupling occurred during consecutive theta cycles in the maintenance period. Power values in a range of 1–50 Hz are triggered to the peak of consecutive theta cycles. Data were first averaged across all trials in each patient, and then averaged across all patients. The vertical axis represents frequency (between 1 and 50 Hz) in each cycle. The horizontal axis is plotted in units of time because we extracted power values from −75 ms to +75 ms triggered to the peak of the consecutive theta cycles (on average, −75 ms and +75 ms correspond to the troughs and 0 ms to the peak of theta band activity).

and Fig. 1*D*). Again, we found that modulation was significantly reduced as compared to the empirical data ($p_{corr} < 0.05$). However, we did observe some degree of modulation in both types of surrogates as well. In principle, this could be due to the fact that gamma power time series are conserved in these surrogates (as well as in the phase-scrambled surrogate data), and that gamma power time series fluctuate in the theta frequency range. In other words, if the frequency spectrum of gamma power time series showed a peak in the theta range, this peak would be conserved in the surrogates. Thus, some degree of cross-frequency coupling would be expected even in the surrogates, in particular in combination with the increased phase locking of theta band activity at the beginning of each trial (Fig. S5*G*). Indeed, we observed such a peak of the gamma power time-series fluctuation in the theta range (Fig. 1*E*).

From Fig. 1*A*, it appears that cross-frequency modulation is also increased in a lower range (between 1 and 4 Hz for the modulating frequency and 14 and 20 Hz for the modulated frequency, resulting in delta-beta coupling). We thus analyzed modulation in these frequency ranges. However, average modulation in these ranges did not differ from modulation during the baseline period ($p_{corr} > 0.5$).

The amplitude of the modulated high-frequency oscillations was concentrated at a phase of 0° of the modulating lower-frequency oscillations (Fig. 1*F*), consistent with data from the hippocampus of awake behaving rats (16). Previous studies have shown that stimulus-induced gamma band activity may appear at specific latencies (18, 23–26). If these gamma band responses occur in combination with an increased phase locking of theta band activity, gamma band responses would be observed at specific theta phases despite the lack of an inherent relationship between gamma power and theta phase. In other words, it might be suspected that apparent cross-frequency coupling may result from a combination of an event-related gamma response and an increased theta phase locking—that is, a gamma power increase and a theta phase locked to the last items in the memory list. Several control analyses were conducted to exclude this possibility. First, we directly investigated event-related spectral perturbations (ERSPs) and intertrial phase coherence (ITC; i.e., phase locking across trials) and compared them to baseline. [Note that an analysis of load effects on ERSPs in a subgroup of 11 out of the entire group of 14 patients was reported in our previous article (7). This analysis did not reveal any significant differences between load conditions; however, a direct comparison with activity in the intertrial interval was not conducted in that study.] These results are shown in Fig. S5 *F* and *G*, and a detailed description of how these measures were calculated is given in *SI Methods*. Visually, we ob-

served an increase in power and ITC at the beginning of the maintenance phase as compared to baseline, which was not apparent during the later maintenance phase. We thus separately compared ERSPs and ITC values during the first and second parts of the maintenance phase with values during the first and second parts of the baseline period (both for maintenance and baseline, two consecutive nonoverlapping parts of 1750 ms). T tests comparing power values at 28 Hz or averaged across the range of 14–50 Hz during maintenance and baseline were not significant, neither in the early nor in the late maintenance phase (all $t_{13} < 1.4$; all $P > 0.1$). Power values at 7 Hz were in trend increased during the early maintenance phase ($t_{13} = 1.99$; $P = 0.07$), but not during the late phase ($t_{13} = 0.02$; $P = 0.99$). Similar results were obtained for the ITC values: Whereas there was a significantly increased phase locking at 7 Hz during the early maintenance phase as compared to the early baseline period ($t_{13} = 4.10$; $P < 0.005$), but not during the respective late phases ($t_{13} = 0.80$; $P = 0.44$), no significant differences were found at 28 Hz or at the averaged values between 14 and 50 Hz (all $t_{13} < 1.4$; all $P > 0.1$). The increased theta power and phase coherence during the early maintenance period probably reflect the stimulus-related hippocampal P300-like components described in our previous study (7).

Next, we conducted the same analysis of cross-frequency modulation as for the entire period in the two parts of the maintenance period. Results in both parts—also in the latter one where no significant ERSPs or increases of ITC were observed—were qualitatively identical to our findings from the entire period (*SI Results* and Fig. S5 *D* and *E*). As differences of power and ITC values between maintenance and baseline were only observed during the first, but not the second, half of the maintenance phase, cross-frequency coupling during the late maintenance phase cannot be explained by task-related effects on event-related power or ITC.

As a second control analysis, we separately analyzed gamma power across each consecutive individual theta cycle during the maintenance period. Figure 1*G* depicts time-frequency plots of power values between 1 and 50 Hz triggered to the peak of each of 20 consecutive (nonoverlapping) theta cycles. Gamma power was modulated at 0° during the majority of theta cycles. To quantify this result, we calculated distributions of gamma power (at 28 Hz) across the consecutive theta cycles (Fig. S6). Please note that in these distributions, the power value at +180° of cycle n is not temporally adjacent to the power value at −180° of the same cycle, but to the value at −180° of cycle n+1. We computed Rayleigh tests of nonuniformity for each cycle, which compare the length of the modulation vectors of these empirical distributions to the modulation vectors of 1000 shuffled surrogate distributions (see *SI Methods*). We found that the distributions differed significantly from uniform distributions in all 20 cycles.

Although oscillations in the theta frequency range are commonly observed in the hippocampus of rodents (27, 28), previous intracranial EEG recordings in the hippocampus of human subjects yielded mixed results: Some researchers failed to find oscillatory activity (indicated by a clear peak in the power spectrum) in the theta frequency range (e.g., ref. 29). Cantero and colleagues (30) observed brief bursts of theta band activity, corresponding to a peak in the power spectrum at 5–6 Hz, specifically during REM sleep and awakenings from sleep. Task-dependent modulations of theta oscillations such as phase locking (31) or amplitude increases (32) suggest a functional role of this activity. In the unfiltered raw data, we observed both slow oscillations in the theta frequency range and faster oscillatory activity in the gamma band (Fig. 2*A*). We found an increased amplitude of beta/gamma band activity around the peak of theta oscillations in individual trials of the filtered hippocampal EEG (7 Hz and 28 Hz; Fig. 2*B*; same trial as shown in Fig. 2*A*). Figure 2*C* depicts a histogram of gamma power values averaged across all trials and patients. Furthermore, there was a peak at around 8 Hz in the grand average power spectrum (Fig. 2*D*). We did not observe a peak in the beta/gamma frequency around 28 Hz. This

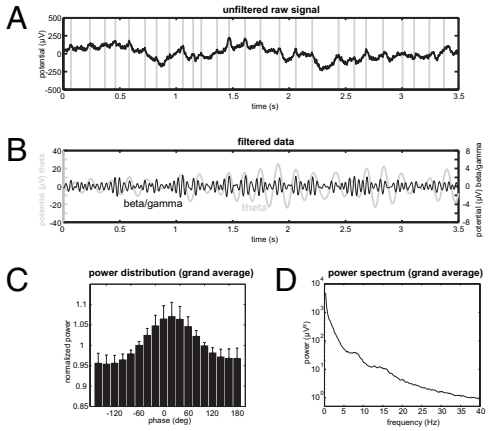

Fig. 2. Time-domain data and grand average of power data. (*A*) Unfiltered raw data in a single trial indicate both slow and fast oscillatory activity. Vertical gray lines indicate visually detected maxima of slow activity. (*B*) Modulation of beta/gamma by theta phase in the same trial filtered at 7 Hz and 28 Hz. (*C*) Grand average of the distribution of beta/gamma power at 28 Hz across all theta phases at 7 Hz. Error bars depict SEM. (*D*) Grand average of the power spectrum shows a peak in the theta frequency range between 7 and 8 Hz.

may indicate that oscillations in this frequency range can only be detected if different phases of simultaneous theta oscillations are distinguished, as in the analysis of cross-frequency coupling.

Next, we compared effects during maintenance of different numbers of items (Fig. 3). Task performance dropped significantly with memory load (proportion of correct trials during load 1, mean ± SEM: 0.8043 ± 0.0351; load 2: 0.7814 ± 0.0298; load 4: 0.6843 ± 0.0481; parametric analysis: $t_{13} = 3.082$; $P < 0.01$). The peak of the lower (modulating) frequency decreased significantly with load from 7.50 ± 0.39 Hz (mean ± SEM) to 6.43 ± 0.20 Hz, as indicated by a significant linear regression (Fig. 3*B*; $t_{13} = 2.583$; $P < 0.05$). Values from individual patients are indicated by colored dots; the number of dots is smaller than the number of patients because of identical values in some patients. In contrast, there was no significant effect of load on the peak of the high (modulated) frequency (Fig. 3*C*; $t_{13} = 1.287$; $P = 0.221$). In detail, the modulated beta/gamma frequency was 30.29 ± 3.13 Hz during maintenance of one item and 25.00 ± 2.62 Hz during maintenance of four items (values for the maximal modulation frequencies of all individual subjects are listed in Table S2). Thus, on a descriptive level, the average values for the modulated beta/gamma frequency were higher during maintenance of one item as compared to maintenance of four items, but due to the high interindividual variability there was no significant frequency change on a group level. The frequency ratio of modulating and modulated activity remained constant at ∼4 across the different load conditions (Fig. 3*D*; $t_{13} = 0.545$; $P = 0.595$). To exclude that these effects were due to differences in power, we compared the power of theta and beta/gamma band activity as a function of memory load (see spectra in Fig. 3*E*). We found that power did not depend on WM load at either 7 Hz ($t_{13} = 0.689$; $P = 0.503$) or 28 Hz ($t_{13} = 0.840$; $P = 0.416$; Fig. 3*F*).

Then, we tested whether the phase range during which beta/gamma amplitude was modulated by theta phase (modulation width; see *Methods*) changed with load. Based on theoretical work (14, 22), we wondered whether beta/gamma oscillations occurred in a more extended theta phase range when more items are maintained. However, modulation width did not depend on memory load (Fig. 4*A*; $t_{13} = 1.30$; $P = 0.218$). On the other hand, the circular variance of the distributions of modulation phases across trials decreased with load (Fig. 4*B*; $t_{13} = 3.986$; $P < 0.005$), indicating that modulation occurred at more specific theta phases with increasing load. Modulation strength was not significantly altered with load (Fig. 4*C*; $t_{13} = 1.315$; $P = 0.211$).

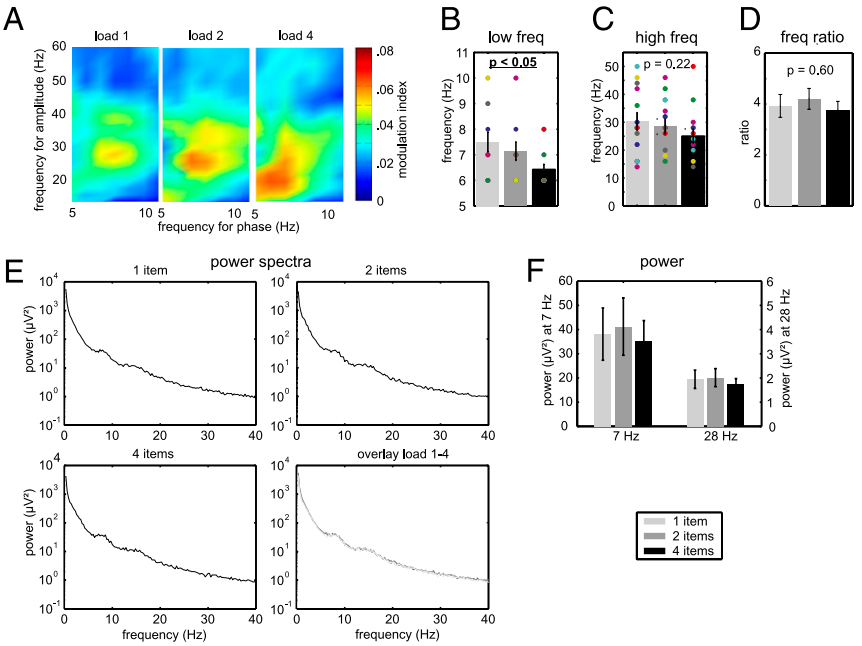

Fig. 3. Modulation frequency depends on working memory load. (*A*) Cross-frequency coupling in the different load conditions. (*B*) The frequency of modulating theta oscillations shifts toward lower frequencies with increasing memory load (colored circles indicate values for individual subjects). (*C*) In contrast, there was no significant change of the modulated frequency due to high interindividual variability. (*D*) Constant ratio of modulating and modulated frequency. Similar power spectra (*E*) and constant power at 7 Hz and 28 Hz (*F*) in the different load conditions. Error bars indicate SEM.

A causal role of hippocampal cross-frequency coupling would suggest that task performance should improve when modulation of beta/gamma by theta oscillations is more precise, that is, when modulation width decreases. Indeed, we observed that better performance (measured as faster reaction times) was interindividually correlated with narrower modulation width in the load 1 condition (Fig. 4*D*; Spearman's correlation coefficient: $R = 0.68$; $t_{13} = 3.24$; $P = 0.007$), but not the other load conditions ($P > 0.6$).

Discussion

We found that cross-frequency coupling of beta/gamma amplitude to theta phase (at a cosine phase value around 0°, so that 0° corresponds to the peak) was more pronounced during WM maintenance as compared to baseline and to phase-scrambled and trial-shuffled surrogates. Increased WM load induced a shift of the (modulating) theta frequency toward lower values and a decreased variance of modulation phases across trials. Moreover, a narrower modulation width predicted faster performance of the WM task in the load 1 condition, suggesting a behavioral relevance of phase-amplitude coupling. These findings demonstrate that cross-frequency coupling in the human hippocampus accompanies WM maintenance.

Recently, the role of the medial temporal lobe (MTL) (and in particular the hippocampus) for WM has been a matter of intense debate. Earlier studies on patients with MTL lesions using relatively simple WM paradigms such as delayed-matching-to-sample tasks did not find any impairment in performance and therefore concluded that the MTL is not required for WM maintenance (33). However, more recent experiments involving multiple items (34) or relations between item features (20, 35) did find impairments in such patients. Similarly, functional MRI studies in healthy control subjects (36) and intracranial EEG studies in epilepsy patients (7) reported that the MTL is involved in WM operations if multiple items or conjunctions of item features are processed. These results support the relational memory theory, which suggests that the hippocampus is ideally suited for memory processes involving multiple items or associations (37, 38). Our results confirm this notion, but move beyond it by providing specific insight into the neural dynamics reflecting hippocampal WM maintenance.

Coupling of beta/gamma amplitude to theta phase was significantly more pronounced during WM maintenance than baseline and compared to phase-scrambled and to trial-shuffled surrogates (Fig. 1), suggesting a functional relevance of this electrophysiological phenomenon. It should be noted, however, that the correlations of beta/gamma power with theta phase described here—the finding that beta/gamma power is "modulated" by theta phase—do not indicate that low frequencies are causally driving the high frequencies. Our results complement previous findings that firing of action potentials at specific phases of lower-frequency oscillations carries information beyond rate coding. In the hippocampus of rodents, spatial positions are not only represented by the firing rate of hippocampal place cells but also—and even more precisely—by the alignment of place cell firing to specific phases of theta band activity (11). In contrast to the well-established encoding of information by firing rate, this mechanism relies on the exact timing of neural activity (39, 40) and is possibly linked to the induction of synaptic plasticity determined by the phase of oscillatory activity (41–44). In addition to action potentials, high-frequency oscillations in the gamma range also are locked to the phase of lower-frequency activity. In the hippocampus (16) and entorhinal cortex (45) of rodents, gamma is typically present only at specific phases of theta band activity. In humans, we have previously investigated synchronization of theta phase and the power of activity in higher-frequency ranges during a continuous recognition paradigm (18). Canolty and colleagues (19) used a similar approach to the one employed in the current study and found that in the neocortex, gamma power was enhanced at the trough of theta

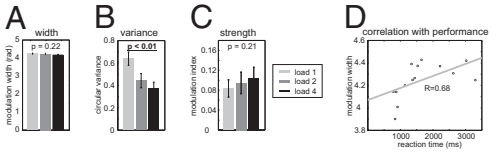

Fig. 4. Properties of cross-frequency coupling for multiple items and relationship with behavior. Effect of load on modulation width (*A*), circular variance of the distributions of modulation phase across trials (*B*), and modulation strength (*C*). (Circular variance and modulation strength are dimensionless quantities.) Modulation width was negatively correlated with the number of correct trials over subjects in the load 1 condition, indicating that modulation in a narrower phase range predicts faster reactions times during working memory (*D*). Error bars indicate SEM.

oscillations during various cognitive tasks. Furthermore, a recent study revealed stimulus-specific enhancements of gamma band activity, which was again increased during the trough of theta oscillations (26); the majority of recording sites in this study were again from the neocortex. In contrast, our recordings from the hippocampus revealed an increased gamma amplitude at the peak of theta oscillations (Fig. 1 *D* and *E*). Thus, whereas gamma amplitude is modulated by theta phase both in the neocortex and in the hippocampus, the theta phase associated with the maximal gamma power appears to differ between structures. This discrepancy may be explained by the different cellular architecture of hippocampus and neocortex and by the unique mechanisms underlying hippocampal theta band activity (28, 46), which leads to a relatively low correlation of hippocampal and neocortical theta band activity during waking state (47). To our knowledge, no previous data exist on the phase of cross-frequency coupling in the human hippocampus. However, Bragin and colleagues (16) described an increased amplitude of gamma band activity at the positive phase of theta oscillations in the hippocampus of awake behaving rats, consistent with our results; similar results were obtained in the mouse hippocampus (48). Our results differ from those of Cantero and colleagues (30), who did not find a modulation of gamma power by theta phase. However, in that study, only three patients with hippocampal depth electrodes were included. Even more important, these patients did not engage in a WM task; therefore, the reported hippocampal activity during waking state is more likely to correspond to the baseline periods in our study, where no significant modulation (as compared to surrogate data) was observed ($p_{corr} > 0.5$).

So far, no study has investigated cross-frequency coupling during WM maintenance with respect to memory load. This is particularly interesting, because theoretical work related to the proposed model has resulted in very specific predictions, namely that individual WM items are represented by consecutive gamma cycles nested in the theta rhythm (14, 15). Functionally, encoding of consecutive items in a sequence prevents collapsing of features from separate items and preserves order information. In this context, the load-dependent decrease of intertrial variance of modulation phase (Fig. 4*B*) might indicate that during simultaneous maintenance of multiple items, each item representation is restricted to a specific narrow phase range. It is likely that maintenance of multiple items requires that each item be processed during a narrower phase range, that is, that the precision of item representations increases. As mentioned in the Introduction, the analyses presented here are based on an extension (14 instead of 11 subjects) of a data sample described in an earlier paper (7). In this previous article, we reported load effects on hippocampal event-related potentials and on event-related spectral perturbations during the maintenance phase. Maintenance of a single item was associated with a sustained reduction of high (>50 Hz) gamma band activity as compared to a prestimulus baseline, whereas no changes were observed in other frequency bands. However, consistent with the current analyses, we did not observe an effect of memory load on hippocampal ERSPs in any frequency range.

The decrease of theta frequency with load (Fig. 3*A* and *B*) has been proposed as a feature supporting multi-item WM maintenance (22). This model framework predicts that working memory representations are maintained by sequential activation of individual items repeated every theta cycle. Thus, the more items maintained, the longer the theta cycle, resulting in a frequency decrease. However, the frequency ratio of beta/gamma to theta oscillations across memory load was constant at ∼4 (Fig. 3*D*): Even though the frequency of modulated beta/gamma band activity did not change significantly with load due to the high interindividual variance (Fig. 3*C*), the average values decreased from around 30 Hz to 25 Hz. This finding contradicts the idea that an increasing number of items can be maintained by locking to consecutive phases of longer theta cycles, and in this respect is not consistent with the model suggested by Jensen and Lisman (22). This constant frequency ratio is consistent with proposals that the number of gamma oscillations per theta cycle determines the WM span, which is around four for complex items such as faces. Further studies with other item types exhibiting a different WM span are necessary to test this idea. For example, it would be ideal to investigate maintenance of a variable number of simple items such as digits or letters for which WM capacity is higher; using our approach, we would predict an increase in the frequency ratio between beta/gamma and theta oscillations for these items.

With increasing load, modulation width remained constant (Fig. 4*A*) but intertrial variance decreased (Fig. 4*B*). Functionally, these effects make sense in the framework of encoding of individual items by consecutive gamma cycles: If individual items are represented by separate gamma cycles, a constant modulation width across the different load conditions can only be explained if the intertrial variance decreases with load; otherwise, the enhanced number of gamma cycles with increasing load would invariably lead to larger modulation widths. Fig. S7 schematically displays this idea.

We found that subjects with a lower modulation width in the load 1 condition (i.e., with a narrower range of theta phases during which beta/gamma amplitude was concentrated) performed significantly faster in the Sternberg task in this condition (Fig. 4*D*). It is possible that a relatively narrow modulation width within each cycle was necessary to keep item representations in consecutive theta cycles apart. This may help to avoid confusion of item representations by beta/gamma cycles in consecutive theta cycles. Taken together, whereas oscillations in different frequency ranges have usually been studied in isolation, our findings demonstrate that understanding cross-frequency coupling is required to elucidate the dynamics of memory processing in the human brain.

Methods

Additional details on patients' characteristics, recordings, and the experimental paradigms can be found in *SI Methods*. In brief, for each patient, data from the hippocampal contact with the maximal slope of the direct current (DC) potential were analyzed because we attempted to capture task-related activity, and DC potentials likely correspond to working memory maintenance (7).

Experimental Paradigm. We used a Sternberg paradigm with serial presentation of items allowing for parametric modulation of the WM load, that is, the number of items to be maintained in the retention interval. Subjects had to memorize one, two, or four black and white photographs of unknown male and female faces that had previously been rated by a large group of subjects as neutral with respect to facial expression. Fig. S1 illustrates the paradigm. Only correct response trials were considered in the analyses.

Analyses of Cross-Frequency Coupling. Cross-frequency coupling was specified by the following approach. First, the average phase $\varphi(\bar{z})$ of the lower-frequency oscillation corresponding to a maximum amplitude of the high-frequency oscillation was estimated according to a previously suggested method (19) (for details, see below). Then, the lower-frequency oscillation was shifted by $-\varphi(\bar{z})$ and Pearson's cross-correlation between the real part of the lower-frequency oscillation and the instantaneous amplitude of high-frequency oscillation was quantified. The rationale underlying this approach was to eliminate the impact of high-frequency amplitude on coupling strength. Furthermore, the shift of the lower-frequency oscillations by $-\varphi(\bar{z})$ guarantees that the maximum cross-correlation is calculated. Otherwise, modulation strength would be affected by the phase offset between the real part of the lower-frequency oscillation and the amplitude of the high-frequency oscillation.

In detail, from the wavelet-transformed signals $w_{j,k}$, the phases $\psi_{j,k}$ ($\psi_{j,k} = \arctan(\mathrm{Im}(w_{j,k})/\mathrm{Re}(w_{j,k}))$) and the amplitude values $A_{j,k}$ ($A_{j,k} = (\mathrm{Re}(w_{j,k})^2 + \mathrm{Im}(w_{j,k})^2)^{0.5}$) were extracted for each time point j of each trial k (number of trials: n). Now, a new complex signal z was composed consisting of the phases ψ_{LF} of the wavelet-transformed signals for lower frequencies between 1 and 14 Hz and the amplitude A_{HF} of the wavelet-transformed signals for high frequencies between 14 and 200 Hz ($z = A_{HF}\, e^{i\psi_{LF}}$) (19). Then, the average complex values $\bar{z}_k$ across all time points of each trial were calculated and the corresponding phases φ_k ($\bar{z}_k$) were extracted ($\varphi_k = \arctan(\mathrm{Im}(\bar{z}_k)/\mathrm{Re}(\bar{z}_k))$). Furthermore, the average complex value $\bar{z}$ across all trials was calculated ($\bar{z} = 1/n \sum \bar{z}_k$) and again the corresponding phase $\varphi(\bar{z})$ was extracted, yielding the *modulation phase*. This value quantifies the average phase of the lower-frequency oscillation at which the amplitude of the high-frequency oscillation is strongest. However, the modulation phase $\phi(\bar{z})$ does not specify how

broadly the phases φ_k ($\bar{z}_k$) are distributed across trials or, in other words, how stable the modulation phase is. To determine the stability of the modulation phase, we quantified the *modulation variance* υ by calculating the circular variance of the distribution of the phases φ_k ($\bar{z}_k$) across trials ($\upsilon = |\sum e^{i\,\varphi k}|$).

Subsequently, we quantified the *modulation strength* μ_k by calculating Pearson's cross-correlations between the real part $Re(w_{LF}^S)$ of the lower-frequency oscillation shifted by $-\varphi(\bar{z})$ and the amplitude A_{HF} of the high-frequency oscillation. It should be noted that in order not to introduce a bias in favor of an apparently stronger modulation, the modulation phase used for this shift was quantified based on all trials and conditions per subject. In other words, the same phase value was used for all trials in a given subject. Values of modulation strength were Fisher-z-transformed to assure normal distribution. Finally, modulation strength values for all trials m of a certain WM-load condition were averaged in each subject. For statistical comparison of cross-frequency coupling during maintenance, baseline (intertrial interval) and for surrogate data, we did not compare modulation strength at a single frequency pair but averaged in a wider range where modulation appeared to occur during maintenance upon visual inspection (between 6–10 Hz and 14–50 Hz)—of course, maximal modulation values at individual frequency pairs were considerably larger. Therefore, correction by the number of all possible frequency pairs would be inadequate. We used a correction based on the overall number of possible (low) frequency to (high) frequency clusters of the same size as the selected cluster, which was 5 Hz for the low frequencies (6–10 Hz) and 37 Hz for the high frequencies (14–50 Hz), that is, $5 \times 37 = 185$, resulting in $(14 \times 187)/185 = 14.2 \cong 14$. For analysis of modulation in the delta-beta frequency ranges, frequencies between 1–4 Hz and 14–20 Hz were investigated, resulting in a correction factor of $14 \times 187/(4 \times 7) = 94$; however, the latter result did not even reach significance with a correction factor of 14.

Another interesting parameter is how broadly high-frequency amplitude peaks are extended across one cycle of the lower-frequency oscillation. This parameter may correspond to the representation of multiple WM items by several adjacent gamma cycles superposed on low-frequency cycles (e.g., ref. 14). To estimate *modulation width* ω, the average amplitude of the high-frequency oscillations across all time points and trials of the respective condition was calculated for different phases of the lower-frequency oscillations. For this purpose, the phase range between $-\pi$ and π was divided into 200 phase bins and amplitude histograms were calculated. Then, the interval encompassing 68% (σ interval) of the total cumulative amplitude on the phase axis centered around $\varphi(\bar{z})$ was determined. For statistical purposes, modulation width during each memory load condition was normalized by the average modulation width in each subject. The consecutive steps of our analysis are listed in *SI Methods* and graphically depicted in Figs. S2–S4.

Two different kinds of surrogate data were used: Phase-scrambled surrogates (surrogate 1; see *SI Methods*), and trial-shuffled surrogates (surrogate 2), where both gamma power time series and theta phase time series in the individual trials were conserved, but the assignment of trials for amplitude and phase information was randomly shuffled. Surrogates were subjected to the identical procedure as the original data.

ACKNOWLEDGMENTS. This work was supported by Volkswagen Foundation Grant I/79878.

1. Baddeley A (1992) Working memory. *Science* 255:556–559.
2. Herrmann C-S, Munk M-H, Engel A-K (2004) Cognitive functions of gamma-band activity: Memory match and utilization. *Trends Cogn Sci* 8:347–355.
3. Fries P (2005) A mechanism for cognitive dynamics: Neuronal communication through neuronal coherence. *Trends Cogn Sci* 9:474–480.
4. Tallon-Baudry C, Bertrand O, Peronnet F, Pernier J (1998) Induced gamma-band activity during the delay of a visual short-term memory task in humans. *J Neurosci* 18: 4244–4254.
5. Howard M-W, et al. (2003) Gamma oscillations correlate with working memory load in humans. *Cereb Cortex* 13:1369–1374.
6. Palva J-M, Palva S, Kaila K (2005) Phase synchrony among neuronal oscillations in the human cortex. *J Neurosci* 25:3962–3972.
7. Axmacher N, et al. (2007) Sustained neural activity patterns during working memory in the human medial temporal lobe. *J Neurosci* 27:7807–7816.
8. Klimesch W (1996) Memory processes, brain oscillations and EEG synchronization. *Int J Psychophysiol* 24:61–100.
9. Raghavachari S, et al. (2001) Gating of human theta oscillations by a working memory task. *J Neurosci* 21:3175–3183.
10. Klimesch W, Schack B, Sauseng P (2005) The functional significance of theta and upper alpha oscillations. *Exp Psychol* 52:99–108.
11. O'Keefe J, Recce M-L (1993) Phase relationship between hippocampal place units and the EEG theta rhythm. *Hippocampus* 3:317–330.
12. Csicsvari J, Jamieson B, Wise K-D, Buzsáki G (2003) Mechanisms of gamma oscillations in the hippocampus of the behaving rat. *Neuron* 37:311–322.
13. Senior T-J, Huxter J-R, Allen K, O'Neill J, Csicsvari J (2008) Gamma oscillatory firing reveals distinct populations of pyramidal cells in the CA1 region of the hippocampus. *J Neurosci* 28:2274–2286.
14. Lisman J-E, Idiart M-A (1995) Storage of 7 +/– 2 short-term memories in oscillatory subcycles. *Science* 267:1512–1515.
15. Jensen O, Lisman J-E (2005) Hippocampal sequence-encoding driven by a cortical multi-item working memory buffer. *Trends Neurosci* 28:67–72.
16. Bragin A, et al. (1995) Gamma (40–100 Hz) oscillation in the hippocampus of the behaving rat. *J Neurosci* 15:47–60.
17. Tort A-B, et al. (2008) Dynamic cross-frequency couplings of local field potential oscillations in rat striatum and hippocampus during performance of a T-maze task. *Proc Natl Acad Sci USA* 105:20517–20522.
18. Mormann F, et al. (2005) Phase/amplitude reset and theta-gamma interaction in the human medial temporal lobe during a continuous word recognition memory task. *Hippocampus* 15:890–900.
19. Canolty R-T, et al. (2006) High gamma power is phase-locked to theta oscillations in human neocortex. *Science* 313:1626–1628.
20. Olson I-R, Page K, Moore K-S, Chatterjee A, Verfaellie M (2006) Working memory for conjunctions relies on the medial temporal lobe. *J Neurosci* 26:4596–4601.
21. Hannula D-E, Ranganath C (2008) Medial temporal lobe activity predicts successful relational memory binding. *J Neurosci* 28:116–124.
22. Jensen O, Lisman J-E (1998) An oscillatory short-term memory buffer model can account for data on the Sternberg task. *J Neurosci* 18:10688–10699.
23. Başar E, Rosen B, Başar-Eroglu C, Greitschus F (1987) The associations between 40 Hz-EEG and the middle latency response of the auditory evoked potential. *Int J Neurosci* 33:103–117.
24. Kaiser J, Lutzenberger W, Ackermann H, Birbaumer N (2002) Dynamics of gamma-band activity induced by auditory pattern changes in humans. *Cereb Cortex* 12:212–221.
25. Gruber T, Tsivilis D, Montaldi D, Müller M-M (2004) Induced gamma band responses: An early marker of memory encoding and retrieval. *Neuroreport* 15:1837–1841.
26. Jacobs J, Kahana M-J (2009) Neural representations of individual stimuli in humans revealed by gamma-band electrocorticographic activity. *J Neurosci* 29:10203–10214.
27. Grastyan E, Lissak K, Madarasz I, Donhoffer H (1959) Hippocampal electrical activity during the development of conditioned reflexes. *Electroencephalogr Clin Neurophysiol Suppl* 11:409–430.
28. Buzsáki G (2002) Theta oscillations in the hippocampus. *Neuron* 33:325–340.
29. Uchida S, Maehara T, Hirai N, Okubo Y, Shimizu H (2001) Cortical oscillations in human medial temporal lobe during wakefulness and all-night sleep. *Brain Res* 891:7–19.
30. Cantero J-L, et al. (2003) Sleep-dependent theta oscillations in the human hippocampus and neocortex. *J Neurosci* 23:10897–10903.
31. Rizzuto D-S, et al. (2003) Reset of human neocortical oscillations during a working memory task. *Proc Natl Acad Sci USA* 100:7931–7936.
32. Ekstrom A-D, et al. (2005) Human hippocampal theta activity during virtual navigation. *Hippocampus* 15:881–889.
33. Cave C-B, Squire L-R (1992) Intact verbal and nonverbal short-term memory following damage to the human hippocampus. *Hippocampus* 2:151–163.
34. Aggleton J-P, Shaw C, Gaffan E-A (1992) The performance of postencephalitic amnesic subjects on two behavioural tests of memory: Concurrent discrimination learning and delayed matching-to-sample. *Cortex* 28:359–372.
35. Hannula D-E, Tranel D, Cohen N-J (2006) The long and the short of it: Relational memory impairments in amnesia, even at short lags. *J Neurosci* 26:8352–8359.
36. Piekema C, Kessels R-P, Mars R-B, Petersson K-M, Fernández G (2006) The right hippocampus participates in short-term memory maintenance of object-location associations. *Neuroimage* 33:374–382.
37. Cohen NJ, Eichenbaum H, eds (1993) *Memory, Amnesia, and the Hippocampal System* (MIT Press, Cambridge, MA).
38. Eichenbaum H (2004) Hippocampus: Cognitive processes and neural representations that underlie declarative memory. *Neuron* 44:109–120.
39. Engel A-K, König P, Kreiter A-K, Schillen T-B, Singer W (1992) Temporal coding in the visual cortex: New vistas on integration in the nervous system. *Trends Neurosci* 15:218–226.
40. Rieke F, Warland D, de Ruyter van Steveninck R, Bialek W, eds (1997) *Spike: Exploring the Neural Code* (MIT Press, Cambridge, MA).
41. Pavlides C, Greenstein Y-J, Grudman M, Winson J (1988) Long-term potentiation in the dentate gyrus is induced preferentially on the positive phase of theta-rhythm. *Brain Res* 439:383–387.
42. Huerta P-T, Lisman J-E (1993) Heightened synaptic plasticity of hippocampal CA1 neurons during a cholinergically induced rhythmic state. *Nature* 364:723–725.
43. Hölscher C, Anwyl R, Rowan M-J (1997) Stimulation on the positive phase of hippocampal theta rhythm induces long-term potentiation that can be depotentiated by stimulation on the negative phase in area CA1 in vivo. *J Neurosci* 17:6470–6477.
44. Wespatat V, Tennigkeit F, Singer W (2004) Phase sensitivity of synaptic modifications in oscillating cells of rat visual cortex. *J Neurosci* 24:9067–9075.
45. Chrobak J-J, Buzsáki G (1998) Gamma oscillations in the entorhinal cortex of the freely behaving rat. *J Neurosci* 18:388–398.
46. Mormann F, et al. (2008) Independent delta/theta rhythms in the human hippocampus and entorhinal cortex. *Front Hum Neurosci* 2:3.
47. Axmacher N, Helmstaedter C, Elger C-E, Fell J (2008) Enhancement of neocortical-medial temporal EEG correlations during non-REM sleep. *Neural Plast* 2008:563028.
48. Buzsáki G, et al. (2003) Hippocampal network patterns of activity in the mouse. *Neuroscience* 116:201–211.